A Quantitative Model for the Coupled Diffusion of Phosphorus and Point Defects in Silicon

Scott T. Dunham

Electrical, Computer and Systems Engineering Department, Boston University, Boston, Massachusetts 02215

ABSTRACT

In this paper, we develop and analyze models for the coupled diffusion of dopants and point defects, since such models have been observed to display the qualitative aspects of high concentration phosphorus diffusion profiles such as the characteristic "kink and tail." We begin by describing a general model for phosphorus diffusion via dopant/defect pairs assuming local equilibrium for electronic processes, but not for chemical processes. Using this system, along with parameters based on experimental data previously reported in the literature, we test common model assumptions. Our analysis concludes that dopant/defect pairing reactions are near local equilibrium, but that defect recombination reactions are not. We then use a simplified model, based on the assumption that the pairing reactions are near equilibrium to simulate phosphorus profiles. By including diffusion of phosphorus via negatively-charged phosphorus/vacancy pairs, in addition to diffusion via phosphorus/interstitial pairs which dominates in intrinsic materials, we are able to match experimental phosphorus diffusion profiles with surface concentrations ranging from intrinsic to solid-solubility at 900 and 1000°C, while remaining consistent with the broad range of previously observed behavior of phosphorus and point defects in silicon.

The diffusion of substitutional dopants takes place via interactions with point defects (interstitials and vacancies). Most impurities have been reasonably well modeled by systems which consider equilibrium point defect concentrations, but phosphorus has long shown apparently "anomalous" behavior such as "kink and tail" diffusion profiles and "base push" effects. Boron shows some of these effects also, but to a much lesser extent.[1,2] Although a number of models have been proposed to explain these effects, the most commonly used quantitative models are based on vacancy interactions[3] and are inconsistent with a large range of observations which show that phosphorus diffuses primarily with interstitials[4] and that the "base push" and related effects are caused by interstitial supersaturation.[5,6] In addition, these models use a phenomenological approach, with different models for the peak and tail regions, and thus are inadequate for modeling process interactions or two- and three-dimensional effects.

Recently, several authors have observed that the qualitative aspects of the phosphorus kink and tail arise naturally from the coupled dopant/point defect system and have developed models to account for observations of enhanced dopant diffusion.[7-15] All of these proposed models follow the basic formalism laid out by Mathiot and Pfister[7] in which dopants are assumed to diffuse only when paired with point defects. However, they differ dramatically in the assumptions made in simplifying the general system to one which is suitable for numerical solution. For example, Mathiot and Pfister[7] and Orlowski[10] assume that all dopant/defect pairing reactions are near equilibrium, but Frenkel pair generation/recombination is not, Morehead and Lever[8,11] and Rorris *et al.*[14] assume both pairing and Frenkel pair recombination are near equilibrium, while Richardson and Mulvaney[12,13] make neither assumption. In addition, the question remains whether a quantitative model for phosphorus, point defects, and their interactions can be developed within this framework which accounts for high concentration phosphorus profiles over the full range of doping concentrations and is also consistent with other point defect phenomena such as enhanced and retarded diffusion during oxidation or nitridation.

The goal of this paper is to determine appropriate assumptions for modeling of coupled diffusion of dopants with point defects and to develop a system which is capable of quantitatively matching experimental results. We begin by describing a general model for the coupled diffusion of dopants with point defects which includes the reactions of dopant/defect pairs with defects and other pairs, as well as the full set of charge states for both dopants and pairs. Next, we quantify the parameters of that model using published experimental data and simulate the system to assess which of the commonly used assumptions are valid for modeling high-concentration phosphorus diffusion. Based on our results, we generate a simplified model and compare the predictions of that model to experimental data including surface doping concentrations from intrinsic to solid-solubility at 900 and 1000°C. Finally, we end by summarizing our conclusions.

Coupled Diffusion Model

In this section, we describe a model for the coupled diffusion of dopants with point defects which represents a generalized version of that suggested by Mathiot and Pfister.[7] Throughout, the dopant is assumed to be phosphorus, but other dopants differ only in the parameter values (and charge for acceptors). We consider charge states in a general manner and include the full set of reactions including pair/defect and pair/pair interactions which are often neglected.

The system in which a dopant diffuses via interactions with point defects can be described by a set of reactions. First, there are the dopant/defect pairing reactions

$$P^+ + I^i \leftrightarrow (PI)^{i+1} \quad [1]$$

$$P^+ + V^i \leftrightarrow (PV)^{i+1} \quad [2]$$

where P^+ represents ionized phosphorus atoms, I and V represent interstitials and vacancies, (PI) and (PV) represent dopant/defect pairs, and i represents the charge state of the defect or pair (–, 0, +, etc.). Next, the recombination and generation of Frenkel pairs must be considered

$$I^i + V^j \leftrightarrow (-i-j)e^- \quad [3]$$

In addition, the pairs can interact directly with the opposite type defect to produce a reaction which is equivalent to a pair dissociation followed by defect recombination

$$(PI)^i + V^j \leftrightarrow P^+ + (1-i-j)e^- \quad [4]$$

$$(PV)^i + I^j \leftrightarrow P^+ + (1-i-j)e^- \quad [5]$$

Finally, two opposite type pairs can recombine leaving two unpaired dopant atoms

$$(PI)^i + (PV)^j \leftrightarrow 2P^+ + (2-i-j)e^- \quad [6]$$

These final three reactions provide an alternative path for the recombination and generation of vacancies and interstitials and have the potential to significantly increase the effective recombination rate for Frenkel pairs at high dopant concentrations as noted by Morehead and Lever.[11]

There are also ionization or charge exchange reactions for each of the charged species. Because electronic interactions are much faster than the atomic diffusion processes, we will assume that all of the ionization reactions are near equilibrium. Thus, for example, the concentrations of interstitials and phosphorus/interstitial pairs in the various charge states are given by

$$C_I^i \cong K_I^i \left(\frac{n_i}{n}\right)^i C_I^0 \quad [7]$$

and

$$C_{(PI)^{i+1}} \cong K_{PI}^{i} \left(\frac{n_i}{n}\right)^{i} C_{(PI)^+} \quad [8]$$

where the Ks represents equilibrium constants. Note that we reference the charge states of the pairs to the positive dopant/defect pair, which corresponds to the pairing of an ionized dopant with a neutral defect.

For our analysis, we assume that there is local charge neutrality and complete impurity ionization. We also ignore band-gap narrowing effects and use Boltzmann statistics. In addition, we assume that charged defects and pairs can be ignored in determining the Fermi level. These assumptions allow us to write the electron concentration n and electric field $\mathscr{E}$ simply in terms of the doping density

$$n \cong \frac{1}{2}\left(C_{P^+} + \sqrt{C_{P^+}^2 + 4n_i^2}\right) \quad [9]$$

$$\mathscr{E} \cong \frac{kT}{q} \nabla \left[\ln\left(\frac{n}{n_i}\right)\right] \quad [10]$$

There are a couple of other simplifying assumptions which have been commonly made in the literature. First, it is often assumed that the dopant/defect pairing reactions are near equilibrium,[7-11,16] which implies that

$$C_{(PI)^{i+1}} \cong K_{P/I}^{i} C_{P^+} C_{I^i} \cong K_{P/I}^{i} K_{I}^{i} \left(\frac{n_i}{n}\right)^{i} C_{P^+} C_{I^0} \quad [11]$$

where $K_{P/I}^{i}$ is the equilibrium constant for the pairing of phosphorus with interstitials in charge state i (Eq. 1). An equivalent expression can be written for vacancy pairing. Another assumption sometimes used in modeling coupled diffusion is that the defect recombination reactions are also near equilibrium[8,11,14,15]

$$C_I C_V \cong C_I^* C_V^* \quad [12]$$

We will begin without making these last two assumptions and use the more general analysis to assess whether these assumptions appear to be justified given parameter values calculated from published experimental data.

Since the charge exchange reactions are assumed to be near equilibrium, the relative numbers of species in each of the charge states depends only on the electron concentration or Fermi level position. Therefore, we can write expressions for the net rate of the pairing and recombination reactions summed over all the charge states. The net rates of the pairing reactions (Eq. 1 and 2) are

$$R_{P/I} = \sum_i k_{P/I}^{i} \left[C_{P^+} C_{I^+} - \frac{C_{(PI)^{i+1}}}{K_{P/I}^{i}}\right] = \left[\sum_i k_{P/I}^{i} K_I^i \left(\frac{n_i}{n}\right)^{i}\right]\left[C_{P^+} C_{I^0} - \frac{C_{(PI)^+}}{K_{P/I}^{0}}\right] \quad [13]$$

$$R_{P/V} = \left[\sum_i k_{P/V}^{i} K_V^i \left(\frac{n_i}{n}\right)^{i}\right]\left[C_{P^+} C_{V^0} - \frac{C_{(PV)^+}}{K_{P/V}^{0}}\right] \quad [14]$$

where ks represent forward reaction rate coefficients. Note that in deriving Eq. 13 and 14, we made use of relationships which exist between the equilibrium constants we have introduced. Since electronic exchange can occur before or after pairing and equilibrium concentrations are independent of path

$$K_{P/I}^{i} K_I^i = K_{PI}^{i} K_{P/I}^{0} \quad [15]$$

and

$$K_{P/V}^{i} K_V^i = K_{PV}^{i} K_{P/V}^{0} \quad [16]$$

In the remainder of the paper, we will only consider the equilibrium constant for pairing with neutral defects and use Eq. 15 and 16 to substitute for $K_{P/I}^{i}$ and $K_{P/V}^{i}$.

The net rate of Frenkel pair recombination (Eq. 3) is

$$R_{I/V} = \left[\sum_{i,j} k_{I/V}^{i,j} K_I^i K_V^j \left(\frac{n_i}{n}\right)^{i+j}\right][C_{I^0} C_{V^0} - C_I^* C_V^*] \quad [17]$$

Finally, the net rates of the pair/defect and pair/pair reactions (Eq. 4, 5, and 6) are

$$R_{PI/V} = \left[\sum_{i,j} k_{PI/V}^{i,j} K_{PI}^{i} K_V^j \left(\frac{n_i}{n}\right)^{i+j}\right][C_{(PI)^+} C_{V^0} - K_{P/I}^{0} C_I^* C_V^* C_{P^+}] \quad [18]$$

$$R_{PV/I} = \left[\sum_{i,j} k_{PV/I}^{i,j} K_{PV}^{i} K_I^j \left(\frac{n_i}{n}\right)^{i+j}\right][C_{(PV)^+} C_{I^0} - K_{P/V}^{0} C_I^* C_V^* C_{P^+}] \quad [19]$$

$$R_{PI/PV} = \left[\sum_{i,j} k_{PI/PV}^{i,j} K_{PI}^{i} K_{PV}^{j} \left(\frac{n_i}{n}\right)^{i+j}\right] \times [C_{(PI)^+} C_{(PV)^+} - K_{P/I}^{0} K_{P/V}^{0} C_I^* C_V^* (C_{P^+})^2] \quad [20]$$

We observe that by considering all the charge states together, we get effective reaction rates which are functions of the Fermi level.

We also need expressions for the fluxes of mobile species, defects, and pairs. We will assume that the unassociated dopants are immobile and dopant diffusion occurs only via pairs. Once again, because of the assumption of local equilibrium for the different charge states of each species, we only need to consider the total flux for all the charge states combined. The flux of interstitials in each of the charge states can be written in terms of the gradient in the neutral concentration and the electron concentration

$$J_{I^i} = -D_{I^i}\left(\nabla C_{I^i} - \frac{iq\mathscr{E}}{kT} C_{I^i}\right) = -D_{I^i} K_I^i \left(\frac{n_i}{n}\right)^{i} \nabla C_{I^0} \quad [21]$$

where D_{I^i} represents the diffusivity of interstitials of charge state i. Thus the total interstitial flux is

$$J_I = \sum_i J_{I^i} = -\left[\sum_i D_{I^i} K_I^i \left(\frac{n_i}{n}\right)^{i}\right] \nabla C_{I^0} \quad [22]$$

Similarly for vacancies

$$J_V = -\left[\sum_i D_{V^i} K_V^i \left(\frac{n_i}{n}\right)^{i}\right] \nabla C_{V^0} \quad [23]$$

The pair fluxes contain an electric field enhancement term since we consider the positively charged pairs as our reference

$$J_{(PI)} = -\left[\sum_i D_{(PI)^{i+1}} K_{PI}^{i} \left(\frac{n_i}{n}\right)^{i}\right]\left[\nabla C_{(PI)^+} + C_{(PI)^+}\left(\frac{n_i}{n}\right) \nabla \left(\frac{n}{n_i}\right)\right] \quad [24]$$

$$J_{(PV)} = -\left[\sum_i D_{(PV)^{i+1}} K_{PV}^{i} \left(\frac{n_i}{n}\right)^{i}\right]\left[\nabla C_{(PV)^+} + C_{(PV)^+}\left(\frac{n_i}{n}\right) \nabla \left(\frac{n}{n_i}\right)\right] \quad [25]$$

where $D_{(PI)^i}$ and $D_{(PV)^i}$ are the diffusivities of dopant/defect pairs with charge i. As with the reaction rates, we get effective diffusivities that are functions of the Fermi level. If we had instead used the neutral pairs as a reference, the resulting equations would be equivalent, but the dependence of the fluxes on variations in the carrier concentration would be included in the gradients in the concentrations of neutral pairs, rather than in explicit electric field terms.

Once we have the net reaction rates and fluxes, we can easily write the continuity equations for the total concentrations (over all the charge states) of each of the species

$$\frac{\partial C_{P^+}}{\partial t} = -R_{P/I} - R_{P/V} + R_{PI/V} + R_{PV/I} + 2R_{PI/PV} \quad [26]$$

$$\frac{\partial C_I}{\partial t} = -\nabla J_I - R_{P/I} - R_{I/V} - R_{PV/I} \quad [27]$$

$$\frac{\partial C_V}{\partial t} = -\nabla J_V - R_{P/V} - R_{I/V} - R_{PI/V} \quad [28]$$

$$\frac{\partial C_{PI}}{\partial t} = -\nabla J_{(PI)} + R_{P/I} - R_{PI/V} - R_{PI/PV} \quad [29]$$

$$\frac{\partial C_{PV}}{\partial t} = -\nabla J_{(PV)} + R_{P/VI} - R_{PV/I} - R_{PI/PV} \quad [30]$$

Equations 26-30 form the basis of the model for predicting phosphorus and point defect profiles arising from coupled diffusion.

Table I. Parameters used for 1000°C phosphorus diffusion simulations as determined from published experimental results.

Parameter	Value
D_I	1.3×10^{-7} cm^2/s
D_V	1.2×10^{-9} cm^2/s
C_I^* (intrinsic)	2.3×10^{13} cm^{-3}
C_V^* (intrinsic)	2.4×10^{15} cm^{-3}
$D_{(PI)^+} K_{P/I}^0 C_I^0$	9.6×10^{-15} cm^2/s
$D_{(PI)^0} K_{P/I}^0 K_{PI}^- C_I^*$	4.9×10^{-15} cm^2/s
K_I^+	0.53
K_I^-	0.06
K_V^+	0.09
K_V^-	1.52
$K_V^=$	0.11

Quantifying Model

There are a large number of parameters required to quantify the system described in Eq. 26-30. Below we discuss how they may be obtained based on the analysis of previously reported experimental results. The parameter values for 1000°C are summarized in Table I.

Isoconcentration diffusion studies in which dopant diffusivity is measured over a range of constant background doping concentrations can be used to determine the dependence of the effective dopant diffusivity on Fermi level or electron concentration. These experiments enable us to calculate the contribution of the different charge states of the dopant/defect pairs to dopant diffusion; however, the experiments do not distinguish between vacancy and interstitial pair diffusion. Therefore, for each charge state, we can only calculate the sum of the effective dopant diffusivity due to vacancy pairs plus that due to interstitial pairs. We analyzed isoconcentration data[17] to determine these parameters for phosphorus. The experimental data can be accounted for by considering only positively-charged and neutral pairs, with resulting parameter values at 1000°C of

$$(D_{(PI)^+} K_{P/I}^0 C_I^0 + D_{(PV)^+} K_{P/V}^0 C_V^*) = 9.6 \times 10^{-15} \text{ cm}^2/\text{s} \quad [31]$$

$$(D_{(PI)^0} K_{P/I}^0 K_{PI}^- C_I^* + D_{(PV)^0} K_{P/V}^0 K_{PV}^- C_V^*) \left(\frac{n}{n_i}\right) = 4.9 \times 10^{-15} \left(\frac{n}{n_i}\right) \text{ cm}^2/\text{s} \quad [32]$$

The fit to the experimental data can be improved slightly by including negatively-charged pairs; however, there is insufficient data to give more than an upper bound of about 2×10^{-16} cm^2/s for the contribution of negatively-charged pairs to the intrinsic diffusivity. Later in this paper, we include negatively-charged phosphorus/vacancy pairs in matching a simplified model to experimental profiles. Since the isoconcentration data do not allow us to determine the concentration of pairs and their diffusivities independently, we assume that the diffusivities of the pairs are independent of their charge state. As we discuss in the following section, the simulation results are nearly independent of the values chosen for the pair diffusivities, as long as the products of pair diffusivity and the equilibrium pair concentration are kept constant.

The relative importance of interstitial *vs.* vacancy pair diffusion can be determined by experiments which use oxidation or nitridation to alter the point defect concentrations. From such experiments, it is found that phosphorus diffuses primarily via interstitial mechanisms under intrinsic conditions.[4] We will therefore neglect diffusion via phosphorus/vacancy pairs in our initial simulations, although diffusion with vacancies is likely to be more significant in heavily doped n-type material and is included in our later simulations.

The locations of defect charge states in the energy gap, which determine the relative numbers of defects in those states as a function of Fermi level, have been calculated for vacancies from electron paramagnetic resonance (EPR) studies[18] and for interstitials from enhanced diffusion in heavily doped material.[19] The defect energy levels can be used to calculate the equilibrium constants for the defect charging reactions which are given in Table I for 1000°C.

The values for the average diffusivity and equilibrium concentration of interstitials and vacancies in intrinsic material have been estimated based on analysis of metal diffusion and silicon self-diffusion.[20,21] The values at 1000°C are listed in Table I. Since there is no experimental determination of the relative diffusivities of the defects in different charge states, we assume the defect diffusivities to be independent of charge state.

In addition to these equilibrium parameters, we need kinetic parameters in order to consider nonequilibrium conditions. We can estimate forward reaction rate coefficients for each reaction from a simple kinetic approximation

$$k_{AB} = 4\pi r (D_A + D_B) \exp\left(\frac{-\Delta E}{kT}\right) \quad [33]$$

where D_A and D_B are the diffusivities of the reactants and ΔE is the energy barrier for the reaction. The upper limit on the reaction rates would be for diffusion limited reactions (no barrier), since an attractive potential would only increase the interaction radius (and only for a long-range potential). As an example, for an interaction radius of $r \cong 5$ Å, the diffusion-limited recombination rate for Frenkel pairs would be $k_{I/V} \cong 8 \times 10^{-14}$ cm^3/s at 1000°C.

Testing of Model Assumptions

Using the partial differential equations and parameter values given in the previous sections, we solve the system numerically using PDECOL, a general partial differential equation solver from the ACM Algorithms Distribution Service.[22] For boundary conditions, we assume a constant phosphorus dose (no flux at surface) and assume that the surface regrowth velocity for both defects is large enough that $C_I \cong C_I^*$ and $C_V \cong C_V^*$ at $x = 0$.

We begin by considering the coupled diffusion of I^0, V^0, $(PI)^+$, and P^+ (a subset of the possible charge states) and the applicable parameters listed in the previous section. We assume that there is no barrier to defect recombination, dopant/defect pairing or dopant-mediated recombination and that the diffusivity of both defects and pairs is independent of charge state. We choose the equilibrium constant for the pairing reaction ($K_{P/I}^0$) such that $D_{(PI)} = D_I$. Figure 1 shows an example of the results of such a simulation for a 5 min diffusion at 1000°C. The resulting phosphorus profile manifests the characteristic kink as well as greatly enhanced diffusion in the tail region. The interstitial and vacancy concentrations are also shown and the interstitial enhancement in the bulk, which gives rise to base push effects is present.

We can also use this simulation to test whether it is appropriate to assume that the pairing reactions and/or recombination reactions are near equilibrium. Figure 1 also plots values of $C_{(PI)^+}/(C_I^0 C_{P^+})$ and $C_I^0 C_V^0$, which should be constant if the associated reactions are near equilibrium. It is clear that, for this system, the pairing reaction is very near local equilibrium for times of interest to very large scale integration (VLSI) fabrication, and thus that Eq. 11 is valid. We conducted additional simulations in which we varied the rate of the pairing reaction and found that $C_{(PI)^+}/(C_I^0 C_{P^+})$ remained nearly constant (less than 10% deviation from equilibrium for all depths during a 5 min diffusion) until the rate of the pairing reaction was reduced by a factor of more than 200 from the diffusion limited rate. On the basis of this and other similar simulations, we conclude that it is reasonable to assume that the dopant/defect pairing reactions are near equilibrium when modeling high concentration diffusion.

In contrast to the pairing reaction, even including pair/defect recombination (or dopant-mediated recombination) and assuming no barrier to recombination and fast surface recombination, the defect recombination process does not

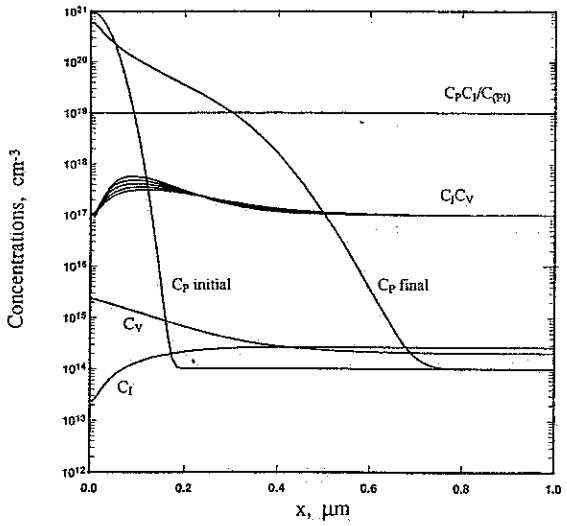

Fig. 1. Simulations of dopant and defect concentrations for simple coupled phosphorus diffusion model after 5 min at 1000°C. Normalized plots of $C_{(PI)^+}/C_IC_{P^+}$ and C_IC_V are used to test whether the pairing and defect recombination reactions, respectively, are near local equilibrium. The initial dopant profile is included for reference.

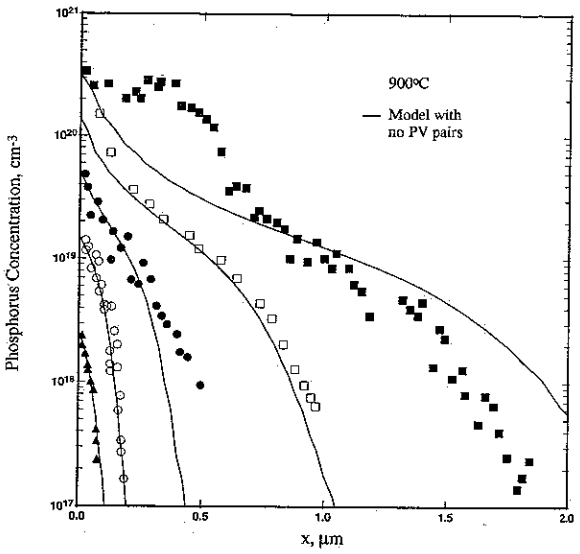

Fig. 2. Active phosphorus concentration profiles based on simulations of diffusion for 4 h at 900°C, neglecting diffusion via PV pairs. The data are as reported by Yoshida *et al.*[41,42] and Matsumoto and Niimi.[43]

appear to be rapid enough to maintain local equilibrium between the defects That is, Eq. 12 does not hold as C_IC_V significantly exceeds $C_I^*C_V^*$ near the kink region where the gradient in dopant and defect concentrations is the greatest, which contradicts the assumption made by Morehead and Lever[8,11] and Rorris *et al.*[14] in their analysis

The conclusion that the Frenkel pair recombination reaction cannot be assumed to be near equilibrium is nearly independent of the value used for $K^0_{P/I}$ over a large range, since it is necessary to keep the $D_{(PI)}K^0_{P/I}$ product fixed in order to account correctly for diffusion in intrinsic material The upper limit on the pair/defect recombination rate is for a diffusion-limited reaction ($\Delta E = 0$ in Eq 33), for which $k_{PI/V} \propto D_{(PI)}$ as long as $D_{(PI)} >> D_V \sim D_I/100$ As the pair density is increased ($K^0_{P/I}$ increased), $D_{(PI)}$, and thus the rate coefficient of the pair/defect recombination reactions, must be reduced proportionately so that the total net recombination rate is unchanged If the barrier for dopant-mediated recombination is much smaller than that for direct Frenkel pair recombination, it is possible for dopant-mediated recombination to greatly increase the effective recombination rate; in that case, however, the rate of direct Frenkel pair recombination must be much slower than the diffusion limited value used in Fig 2, and C_IC_V would deviate even further from the equilibrium product

In previous work, pair/defect reactions or dopant-mediated recombination has been cited as the mechanism by which local equilibrium of the Frenkel pair generation/recombination reaction is maintained during high-concentration diffusion [11,13,14] We can estimate the effectiveness of dopant-mediated recombination in increasing the effective recombination rate by comparing $R_{PI/V}$ to $R_{I/V}$. Assuming that $R_{PI/V}$ and $R_{I/V}$ are limited by the diffusion of pairs and interstitials, respectively, and that the diffusivities and thus recombination rates are independent of charge state

$$\frac{R_{PI/V}}{R_{I/V}} = \frac{D_{(PI)}\left[\sum_i K^i_{PI}\left(\frac{n_i}{n}\right)^i\right] K^0_{P/I}C_I^{*0}C_{P^+}}{D_I\left[\sum_i K^i_I\left(\frac{n_i}{n}\right)^i\right]C_I^{*0}} \qquad [34]$$

Using the parameters in Table I for 1000°C, this ratio is 8 5 at solid-solubility (3.8×10^{20} cm^{-3}) [23] and much smaller for lower concentrations Therefore, it appears that dopant-mediated recombination, although significant, is limited in its ability to enhance recombination Simulations support this conclusion as ignoring pair/defect recombination only slightly alters the simulations shown in Fig 1

For $D_{(PI)} < D_V$, pair/defect recombination becomes limited by the vacancy diffusivity instead of pair diffusivity, and thus for very large values of $K^0_{P/I}$, dopant-mediated recombination can significantly increase the effective recombination rate Simulations show that for dopant-mediated recombination to bring the defects near local equilibrium ($C_IC_V \cong C_I^*C_V^*$), would require a value of $K^0_{P/I}$ large enough that $D_{(PI)} < 2 \times 10^{-5}\, D_I$ and $C_{(PI)} > C_{P^+}/200$. It may be noted that Mulvaney and Richardson[13] assumed that phosphorus/interstitial pairs were slow diffusers (and also that vacancies diffused rapidly) and found that under these circumstances, as discussed above, defect-mediated recombination dramatically increased the effective rate of Frenkel pair recombination

Simplified Model

Since it appears that the dopant/defect pairing reaction is near equilibrium, we can reduce the number of differential equations and parameters needed to describe the system Assuming the pairing reaction (Eq. 11) to be near equilibrium, Eq 26-30 reduce to three continuity equations containing four flux terms and one reaction term

$$\frac{\partial C_P^T}{\partial t} = \frac{\partial(C_{P^+} + C_{(PI)} + C_{(PV)})}{\partial t} = -\nabla \quad (J_{(PI)} + J_{(PV)}) \qquad [35]$$

$$\frac{\partial C_I^T}{\partial t} = \frac{\partial(C_I + C_{(PI)})}{\partial t} = -\nabla \quad (J_I + J_{(PI)}) - R \qquad [36]$$

$$\frac{\partial C_V^T}{\partial t} = \frac{\partial(C_V + C_{(PV)})}{\partial t} = -\nabla \quad (J_V + J_{(PV)}) - R \qquad [37]$$

where C_I, C_V, $C_{(PI)}$, and $C_{(PV)}$ represent the concentrations of point defects and pairs summed over all their charge states and C_I^T, C_V^T, and C_P^T represent the total concentrations of point defect and dopants, both paired and unpaired

The net recombination rate R includes not only normal Frenkel pair recombination, but also pair/defect and pair/pair recombination

$$R = R_{I/V} + R_{PI/V} + R_{PV/I} + R_{PI/PV} \qquad [38]$$

The Frenkel pair recombination rate $R_{I/V}$ remains as given in Eq 17 Using the assumption that the dopant/defect pairing reactions are near equilibrium (Eq 11) we can write the rate of pair/defect and pair/pair recombination (Eq 4-6) in terms of the concentrations of dopants and isolated defect. The total net recombination is then given by

$$R = k_{I/V}\,(C_IC_V - C_I^*C_V^*) \qquad [39]$$

where the effective recombination rate coefficient is

$$k_{I/V} = \frac{\sum_{i,j} [k_{I/V}^{ij} K_I^i K_V^j + (k_{PI/V}^{ij} K_{PI}^i K_{P/I}^0 K_V^j + k_{PV/I}^{ij} K_{PV}^i K_{P/V}^0 K_I^j) C_{P^+} + k_{PI/PV}^{ij} K_{PI}^i K_{PV}^j K_{P/I}^0 K_{P/V}^0 C_{P^+}^2] \left(\frac{n_i}{n}\right)^{i+j}}{\sum_{i,j} K_I^i K_V^j \left(\frac{n_i}{n}\right)^{i+j}} \quad [40]$$

which increases at high doping levels due to pair/defect and pair/pair recombination. The point defect fluxes and pair fluxes as defined in Eq. 22-25 can be rewritten in a similar manner.

The parameters which define this reduced system are the equilibrium constants for the ionization reactions, K_I^i, K_V^i, K_{PI}^i, K_{PV}^i (defined by the location of the defect and pair levels in the bandgap, with K_I^0, K_V^0, K_{PI}^0, K_{PV}^0 equal to unity); the equilibrium constants for the dopant/neutral defect pairing reactions, $K_{P/I}^0$ and $K_{P/V}^0$ (related to the dopant/defect binding energy); the diffusivities of the defects and pairs, D_I^i, D_V^i, $D_{(PI)^i}$, $D_{(PV)^i}$; and the rate coefficients for recombination both direct, $k_{I/V}^{ij}$, and via pairs, $k_{PI/V}^{ij}$, $k_{PV/I}^{ij}$, $k_{PI/PV}^{ij}$.

Equation 35 can be further simplified by assuming that the concentration of pairs remains well below the dopant concentrations and thus $C_P^T \cong C_{P^+}$. In order to justify this assumption, we estimate the pair concentrations by combining measured dopant diffusivity with an estimate of the pair diffusivity. Considering phosphorus for example, if the diffusivity of the dopant/interstitial pairs is the same as the isolated interstitial, then, using the parameters in Table I, $C_{(PI)}/C_{P^+} \cong 10^{-7}$ at equilibrium in intrinsic material and $C_{(PI)}/C_{P^+} < 2 \times 10^{-6}$ at solid-solubility. Thus, pairs can be neglected relative to the doping as long as $(C_I/C_I^*)(D_{(PI)}/D_I) << 5 \times 10^5$. Of course for $C_I >> C_I^*$, as might occur following ion implantation, it may be necessary to account for the reduction in the concentration of isolated dopant atoms due to pairing. In contrast, we cannot ignore the concentration of pairs relative to the unassociated defects. If $D_{(PI)} \sim D_I$, then at solid-solubility $C_{(PI)}/C_I \sim 10$.

An additional complication arises because, at very high doping levels, a portion of the dopant is inactive and/or immobile. In the case of phosphorus, it is believed that precipitation accounts for the inactive phosphorus,[24] but most diffusion models use easier to implement clustering models. Precipitates would be expected to be both inactive and immobile, reducing the carrier concentration and effective dopant diffusion in the peak region. These effects can be accounted for in a straightforward manner by breaking up the dopant concentration into active and inactive precipitated components. Then $C_P^T \cong C_{P^+} + C_P^{ppt}$ and an addition continuity equation is added for the precipitated dopant

$$\frac{\partial C_P^{ppt}}{\partial t} = R_{ppt} \quad [41]$$

where R_{ppt} is the rate of precipitation as a function of C_{P^+}, C_P^{ppt}, C_I^T, and C_V^T. This equation can be subtracted from the C_P^T continuity equation to keep C_{P^+} as a solution variable. However, determining the form of R_{ppt} is a difficult problem which will not be considered in this work, since not only the amount of precipitated material, but also the size distribution of precipitates must be considered for accurate analysis. Therefore, in the next section, we limit our analysis to phosphorus concentrations below solid solubility.

Comparison to Experiment and Discussion

In the remainder of this work, the simulations will utilize the simplified model described in the previous section with solution variables C_{P^+}, C_I, and C_V. These simulations were performed using a modified version of SUPREM IV[16] and thus are incorporated into a system which can model two-dimensional diffusion with multiple dopants and point defect injection processes.

Correctly modeling the changes in diffusion as a function of dose or surface concentrations is one of the most difficult challenges for high concentration diffusion modeling. In contrast to previous comparisons of coupled diffusion models to experimental data,[9-14] we compare our models to experimental profiles over the full range of surface concentrations from intrinsic to solid-solubility using a single set of parameters at each temperature considered. For example, Mulvaney and Richardson[9] compared experimental data to a system which assumed vacancy interactions could be neglected (no PV pairs and no I/V recombination). By adjusting their parameters, they were able to closely match a single profile, but using their model on other data from the same work[25] with different implant doses shows dramatic discrepancies[26] as the experimental results for a higher dose show significant diffusion in the peak region which is not predicted by the model and the model greatly overestimates the tail diffusion.

There has been some disagreement over whether there is a large barrier to I/V recombination. Measurements of enhanced and retarded diffusion during oxidation have resulted in contradictory conclusions. Antoniadis and Moskowitz[27] found apparently slow recombination suggesting a large barrier, while more recent measurements by Guerrero *et al.*[28] suggest that there is at most a small barrier to recombination and local equilibrium between point defects occurs rapidly at diffusion temperatures. In addition, as noted above, at high concentrations, pair/defect reactions provide an alternate path for recombination. We have shown in previous work,[26] and it has also been observed by Richardson and Mulvaney[29] for a similar system, that relatively rapid I/V recombination (small or negligible barrier) is required in order for simulations to approximate experimental profiles. The enhanced diffusion in the tail region is due to the balance of the dissociation of phosphorus/interstitial pairs with the recombination of interstitials with vacancies and/or diffusion of interstitials back to surface. Without strong recombination, the enhancement in the tail region is too large and the kink occurs near the surface, in contrast with experimental observations.

Although observations of enhanced and retarded diffusion during oxidation and nitridation show that the diffusion of phosphorus in intrinsic material is dominated almost totally by interstitial mechanisms,[4] the same is not necessarily true in heavily doped material. Phosphorus/vacancy pairs have been found to have an acceptor level well within the bandgap.[30,31] There is no similar evidence for the existence of negatively-charged phosphorus/interstitial pairs and the evidence that interstitials have only a singly-charged acceptor state in the bandgap[19-32] suggests that only positive and neutral phosphorus/interstitial pairs are present in significant numbers. Since the number of negatively-charged vacancy pairs increases in proportion to the square of the electron concentration, diffusion via negatively-charged vacancy pairs may be dominant near solid-solubility, while contributing less than 2% to diffusion in lightly-doped material.

An additional possibility which should be considered at high doping concentrations once PV pairs are included in the analysis is the interaction of vacancies with more than one dopant atom at a time. In the silicon lattice, in order for a dopant/vacancy pair to diffuse, it is necessary for the vacancy to move away to a third-nearest-neighbor site and return along a different path. The interaction potential between the dopant and the vacancy must therefore extend to at least the third-nearest-neighbor sites in order for dopant diffusion to be faster than self-diffusion (as observed experimentally).[33] In very heavily doped material, as a vacancy moves away from one dopant, it is likely to approach another dopant. The attractive potential between the vacancy and the other dopant can be expected to reduce the activation barrier that the vacancy must overcome in moving to the third-nearest-neighbor site, decreasing the activation energy for pair diffusion and thus increasing the pair diffusivity. Mathiot and Pfister[7,34,35] have calculated

Table II. Optimized parameters for phosphorus diffusion at 900 and 1000°C for the three different model assumptions analyzed. The values given for $D_{(PV)^-}K^0_{P/V}K^-_{PV}C^*_{V^0}$ for the model with concentration-dependent pair diffusivity are with $C_{P^+} = n_i$.

Temperature	Parameter	Optimized Values		
		No PV pairs	$D_{(PV)^-}$ constant	$D_{(PV)^-} \propto C_{P^+}{}^2$
900°C	$D_{(PI)^0}K^0_{P/I}K^-_{PI}C^*_{I^0}$ (cm²/s)	5.3×10^{-16}	7.0×10^{-16}	7.1×10^{-16}
	$D_{(PV)^-}K^0_{P/V}K^-_{PV}C^*_{V^0}$ (cm²/s)	—	1.1×10^{-17}	3.1×10^{-21}
	$k_{I/V}$ (cm³/s)	1.3×10^{-14}	2.7×10^{-14}	3.9×10^{-14}
1000°C	$D_{(PI)^0}K^0_{P/I}K^-_{PI}C^*_{I^0}$ (cm²/s)	6.0×10^{-15}	5.4×10^{-15}	6.3×10^{-15}
	$D_{(PV)^-}K^0_{P/V}K^-_{PV}C^*_{V^0}$ (cm²/s)	—	1.2×10^{-16}	4.6×10^{-20}
	$k_{I/V}$ (cm³/s)	3.3×10^{-14}	1.7×10^{-14}	4.7×10^{-14}

that for doping concentrations above about 3×10^{20} cm^{-3}, the probability of another dopant being close enough to interact with a vacancy at a third-nearest-neighbor site becomes very high. Recent experimental results[36-40] have confirmed that the other common group V dopants (As and Sb), as well as group IV Sn, show anomalously rapid diffusion for donor concentrations above about 2×10^{20} cm^{-3}.

Mathiot and Pfister invoke a percolation phenomena to model the increased dopant diffusivity; however, interactions of vacancies with multiple dopants does not require a critical percolation cluster in order to enhance dopant/vacancy pair diffusivity. As the doping density increases, the average reduction in the activation barrier for pair diffusion reduces, causing an increase in the average pair diffusivity with increased doping concentration. From the analysis of isoconcentration experiments with very high phosphorus background doping,[36-40] it has been observed that dopant diffusivity is proportional to $(C_{P^+})^m$, where $3 < m < 5$, substantially stronger than the $(C_{P^+})^2$ dependence expected for diffusion via negatively-charged pairs. The effect of very high dopant concentrations on the pair diffusivity can be accounted for simply by assuming that the pair diffusivity has a power-law dependence on the carrier concentration. Considering a fourth-power dependence of the dopant diffusivity on the doping concentration, which is typical of the experimental results for other impurities,[36-40] and assuming that the pair is negatively-charged implies that the pair diffusivity depends on the square of the active donor density. This effect can easily be included in the models described above by making the diffusivity a function of the doping concentration in the phosphorus/vacancy pair current equation (Eq. 25).

In order to test the simplified model for coupled diffusion described above, we conducted a series of simulations and compared the results to an extensive series of experimental data reported by Yoshida *et al.*[41,42] and Matsumoto and Niimi.[43] The experimental profiles all resulted from diffusion from SiO_2 doped with various levels of phosphorus and produced surface concentrations that were constant with time. The doping profiles were all measured using differential conductivity and anodic oxidation.

As noted above, published phosphorus isoconcentration data is insufficient to reliably determine the extent to which phosphorus diffuses with negatively-charged pairs and only at 1000°C is there even sufficient data to estimate the contribution due to neutral pairs. Therefore, the values of these parameters were chosen to best match the experimental data. In addition, since there is no accurate estimate of the bimolecular recombination rate, the effective rate of Frenkel pair recombination was also allowed to vary. These parameter values were determined by minimizing the difference between the simulated and measured profiles using a Levenberg-Marquardt optimization code (PROFILE)[44] and the results are summarized in Table II. The rest of the parameters, including all point defect parameters and intrinsic diffusivities are based on the sources cited above.

Our first set of comparisons assumes that diffusion occurs only via positive and neutral interstitial pairs and that vacancy pairs can be neglected (Fig. 2 and 3). This model is similar to that utilized in our previous work[26] and by Richardson and Mulvaney.[12] In both earlier works, a reasonable fit was obtained to a single profile by assuming rapid recombination, but the simulations significantly underestimated diffusion in the peak region. The problem is much more severe when fitting profiles over a range of peak concentrations, and it is clear from Fig. 2 and 3 that without considering phosphorus/vacancy pairs, the coupled diffusion model is unable to account for the experimental results. Note that since the effective recombination rate was optimized to match the data, very fast recombination is insufficient to produce the experimentally-observed high concentration diffusion profiles in contrast to assertions made by Richardson and Mulvaney.[29]

Figures 4-7 show the effects of including diffusion via negatively-charged phosphorus/vacancy pairs. For the simulations shown in Fig. 4 and 5, the diffusivity of $(PV)^-$ pairs was assumed to be independent of doping, while in Fig. 6 and 7, $D_{(PV)^-}$ was assumed to be proportional to the square of the active doping density so that the effective phosphorus diffusivity depended on $(C_{P^+})^4$ at very high concentrations as has been observed for other group IV and V impurities. In both cases, the coupled diffusion model does an excellent job of matching the experimental results over the full range of doping levels. The concentration-dependent pair diffusion slightly improves the appearance of the fits by giving a more pronounced kink for the highest concentrations and a surface kink for the next smaller doping level, but the average errors over the entire set of profiles are nearly the same in the two cases.

For all of the simulations shown in this work, we assumed that interface recombination was rapid enough to

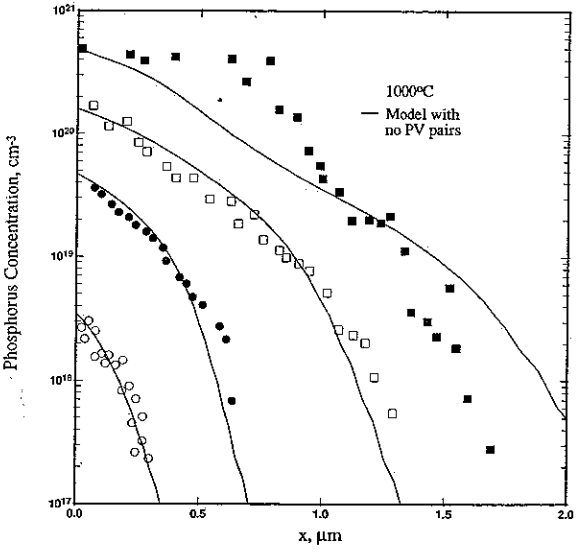

Fig. 3. Active phosphorus concentration profiles based on simulations of diffusion at 1000°C, neglecting diffusion via PV pairs. Diffusion times are 2 h with the exception of the highest dose for which the diffusion time was 1 h. The data is as reported by Yoshida[41] and Matsumoto and Niimi.[43]

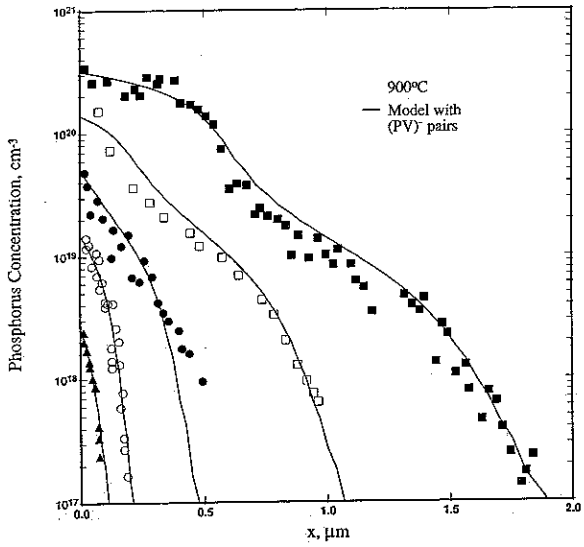

Fig. 4. Active phosphorus concentration profiles based on simulations of diffusion for 4 h at 900°C, including diffusion via $(PV)^-$ pairs. The data are as reported by Yoshida *et al.*[41,42] and Matsumoto and Niimi.[43]

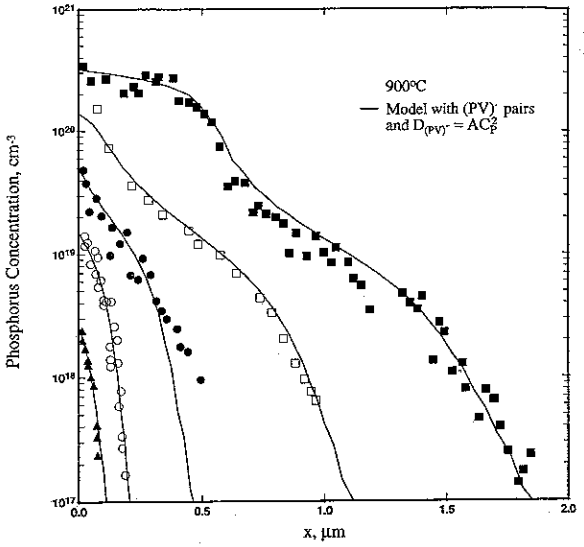

Fig. 6. Active phosphorus concentration profiles based on simulations of diffusion for 4 h at 900°C, including diffusion via $(PV)^-$ pairs and assuming that $D_{(PV)^-} \propto C_P^2$. The data are as reported by Yoshida *et al.*[41,42] and Matsumoto and Niimi.[43]

keep the point defect concentrations near their equilibrium values at the top surface. We also conducted simulations using interface recombination velocities calculated for thermal oxides by Griffin and Plummer.[45] We found that the match to the experimental data was significantly better for the higher recombination velocity. These results suggest that, as would be expected, the effective recombination velocities for the heavily-doped deposited oxides used as doping sources for the experimental data analyzed in this work[39-41] were substantially larger than that typical of thermally grown oxides.

We can make a number of observations from the simulation results. First, the values calculated for $D^0_{(PI)}$ at 1000°C are very similar to those derived from isoconcentration experiments[17] (Table I), supporting the validity of the calculated parameters. Second, based on the parameters listed in Table II, diffusion via $(PV)^-$ pairs does not equal diffusion via $(PI)^0$ pairs until the doping reaches 3 or 4×10^{20} cm^{-3} for both of the models which include $(PV)^-$ pairs. This is consistent with the calculations made by Mathiot and Pfister[34] that the effects of neighboring dopant atoms becomes significant for doping concentrations above about 3×10^{20} cm^{-3}, as well as the experimental results for other impurities.[36-40] Third, the calculated values for effective recombination rate are quite similar to the diffusion-limited values estimated from Eq. 33 (1.3×10^{-14} cm^3/s at 900°C and 8×10^{-3}/s at 1000°C), which implies that there is little or no barrier to Frenkel pair recombination. The recombination rates are large enough to play an important role in determining the diffusion profiles, but as discussed earlier, are not large enough to maintain the Frenkel pair recombination reaction near equilibrium in regions of maximum dopant and defect gradient.

We can consider the role of the Frenkel pair recombination rate in more detail by trying to match this same data using a recombination rate which is fast enough to maintain $C_I C_V \cong C_I^* C_V^*$ throughout the bulk, even in the kink region. Using the model which includes negatively-charged phosphorus/vacancy pairs with constant pair diffusivity (which does an excellent job of matching the ex-

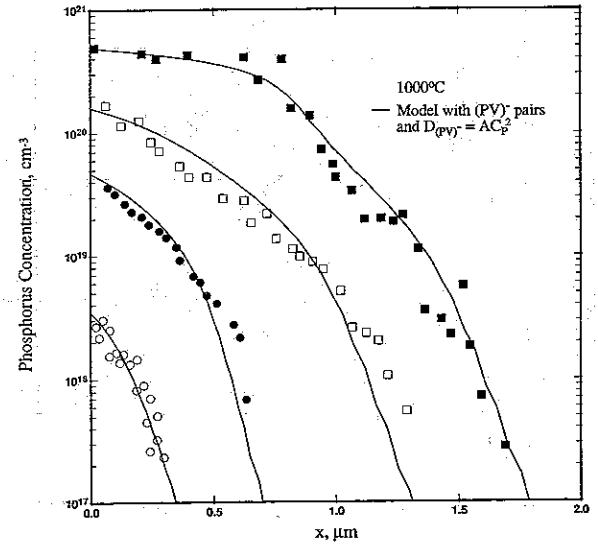

Fig. 5. Active phosphorus concentration profiles based on simulations of diffusion at 1000°C, including diffusion via $(PV)^-$ pairs. Diffusion times are 2 h with the exception of the highest dose for which the diffusion time was 1 h. The data are as reported by Yoshida[41] and Matsumoto and Niimi.[43]

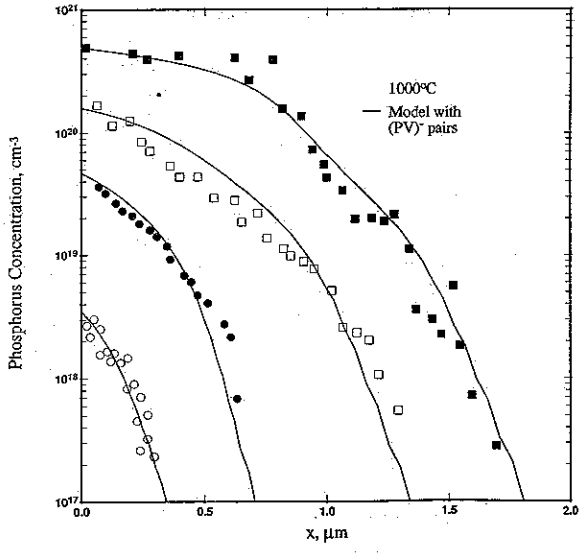

Fig. 7. Active phosphorus concentration profiles based on simulations of diffusion at 1000°C, including diffusion via $(PV)^-$ pairs and assuming that $D_{(PV)^-} \propto C_P^2$. Diffusion times are 2 h with the exception of the highest dose for which the diffusion time was 1 h. The data are as reported by Yoshida[41] and Matsumoto and Niimi.[43]

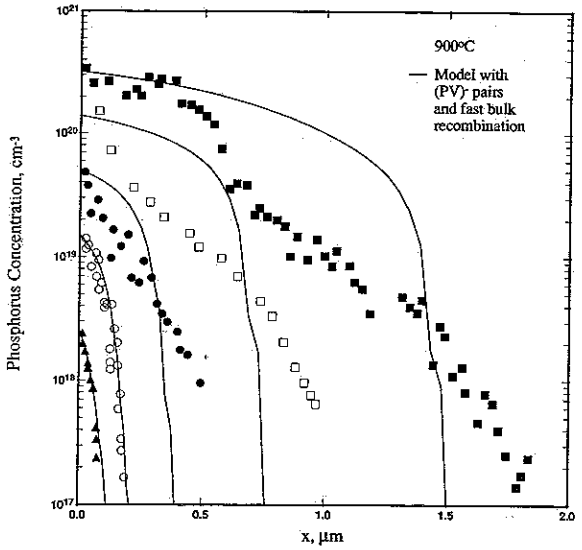

Fig. 8. Active phosphorus concentration profiles based on simulations of diffusion for 4 h at 900°C, including diffusion via $(PV)^-$ pairs and assuming rapid bulk recombination so that $C_IC_V \cong C_I^*C_V^*$. The data are as reported by Yoshida *et al.*[41,42] and Matsumoto and Niimi.[43]

perimental data as shown in Fig. 5 and 6), we increased the recombination rate by over two orders of magnitude (which was large enough so that the C_IC_V product remained within 10% of the equilibrium product for all the profiles). As for previous simulations, the other parameters were optimized to best match the experimental data. It is clear from Fig. 8, which shows the best fit for the 900°C data, that the deviation of C_IC_V from $C_I^*C_V^*$ has a dramatic effect on the doping profiles and that it is not possible to match the experimental results using this model if the recombination rate is assumed to be very large. Just as neglecting bulk recombination greatly overestimated the tail diffusion,[29] assuming very rapid defect recombination greatly underestimates the tail diffusion. By considering negatively-charged phosphorus/interstitial pairs instead of phosphorus/vacancy pairs, it is possible to generate profiles which manifest the characteristic kink and tail features while assuming fast bulk recombination. However, as for the model without vacancy pairs shown in Fig. 2 and 3, even with optimized parameters, the simulations do not correctly account for the changes in profile shape with doping concentration observed experimentally.

Conclusions

In this work, we have developed models for the coupled diffusion of dopants and point defects which can account quantitatively for phosphorus diffusion profiles over the full range of doping levels. Starting with a general model for the coupled dopant/defect system assuming that electronic, but not chemical, processes are near local equilibrium, we simulated the phosphorus system using published values of point defect and dopant parameters combined with estimates of the kinetic parameters. We found that the assumption that dopant/defect pairing reactions are near local equilibrium is justified, but that even with dopant-mediated recombination and with no barriers to recombination, point defect recombination is not fast enough to bring the interstitial and vacancy concentrations to near local equilibrium in regions of large dopant concentration gradient.

Utilizing our conclusion that the dopant/defect pairing reactions remain near equilibrium, we derived a simplified model which we compared to an extensive set of published experimental phosphorus diffusion profiles at 900 and 1000°C. We found that when we included diffusion via negatively-charged phosphorus/vacancy pairs, the model was able to account for the experimental data over the full range of peak doping concentrations, from intrinsic to solid-solubility.

The model was able to match the experimental data both with the diffusivity of $(PV)^-$ proportional to the square of the active doping concentration (as observed at high concentrations for the other common donor impurities) as well as assuming a constant diffusivity for $(PV)^-$ (as in traditional models), but utilizing the concentration-dependent pair diffusivity replicated some of the qualitative features of high-concentration phosphorus diffusion profiles more clearly. Accurate isoconcentration diffusion studies for phosphorus near solid solubility and investigation of diffusion and precipitation at concentrations above solid solubility will be required in order to further evaluate the importance of concentration-dependent phosphorus/vacancy pair diffusivity.

In the analysis, the effective recombination rate for Frenkel pairs was used as an optimization parameter, and the best results were obtained for recombination rates that were similar to those estimated using a simple diffusion-limited kinetic approximation. This result is consistent with recent calculations of the recombination rate based on enhanced and retarded diffusion, which conclude that there is little or no barrier to recombination. Since a constant effective recombination rate was assumed, the results presented here may be improved by consideration of a concentration-dependent recombination rate arising from pair/defect reactions. We also found that using a much higher recombination rate, which was sufficient to keep $C_IC_V \cong C_I^*C_V^*$, resulted in simulated profiles which could not be reconciled with the experimental data.

In summary, the model considered in this paper correctly predicts the rapid diffusion in the peak region observed at high concentrations as well as the dependence of tail diffusion on peak doping level, while remaining consistent with experimental evidence that intrinsic phosphorus diffusion is dominated by interstitials. Since published values for point defect parameters and intrinsic diffusivity are used, the model also is consistent with the broad range of point defect related behavior observed in silicon and appears to have achieved the goal of developing a quantitative model for the coupled diffusion of phosphorus with point defects that is suitable for process simulation applications.

Acknowledgments

This work was supported by a SEMATECH Center of Excellence grant No. 90-MC-503 and NSF grant No. ECS-9009591.

Manuscript submitted March 11, 1992, revised manuscript received May 4, 1992.

Boston University assisted in meeting the publication costs of this article.

REFERENCES

1. S. Matsumoto, Y. Ishikawa, Y. Shirai, S. Sekine, and T. Niimi, *Jpn. J. Appl. Phys.*, **19**, 217 (1980).
2. R. Lever, B. Garben, C. M. Hseih, and W. A. Orr Arienzo, in *Impurity Diffusion and Gettering in Silicon*, Vol. 36, R. B. Fair, C. W. Pearce and J. Washburn, Editors, p. 95, Materials Research Society, Pittsburgh, PA (1985).
3. R. B. Fair, in *Semiconductor Silicon 1977*, H. R. Huff and E. Sirtl, Editors, PV 77-2, p. 968, Electrochemical Society Softbound Proceedings Series, Princeton, NJ (1977).
4. P. Fahey, G. Barbuscia, M. Moslehi, and R. W. Dutton, *Appl. Phys. Lett.*, **43**, 683 (1983).
5. P. Fahey, R. W. Dutton, and S. M. Hu, *ibid.*, **44**, 777 (1984).
6. K. Nishi and D. A. Antoniadis, *J. Appl. Phys.*, **59**, 1117 (1986).
7. D. Mathiot and J. C. Pfister, *ibid.*, **55**, 3518 (1984).
8. F. F. Morehead and R. F. Lever, *Appl. Phys. Lett.*, **48**, 151 (1986).
9. B. Mulvaney and W. Richardson, *ibid.*, **51**, 1439 (1987).
10. M. Orlowski, *ibid.*, **53**, 1323 (1988).
11. F. F. Morehead and R. F. Lever, *J. Appl. Phys.*, **66**, 151 (1989).
12. W. Richardson and B. Mulvaney, *ibid.*, **65**, 2243 (1989).
13. B. Mulvaney and W. Richardson, *ibid.*, **67**, 3197 (1989).
14. E. Rorris, R. R. O'Brien, F. F. Morehead, R. F. Lever,

J P Peng, and G R Srinivasan, *IEEE Trans CAD*, **9**, 1113 (1990)
15 D Mathiot and S Martin, *J Appl. Phys*, **70**, 3071 (1991)
16 M E Law and R W Dutton, *IEEE Trans CAD*, **7**, 181 (1988)
17 J S Makris and B J Masters, *This Journal*, **120**, 1253 (1973)
18 G D Watkins, in *Lattice Defects in Semiconductors 1974*, F A Huntley, Editor, Institute of Physics, London (1975)
19 M D Giles, *IEEE Trans, CAD*, **8**, 460 (1989)
20 G B Bronner and J D Plummer, *J Appl. Phys*, **61**, 5286 (1987)
21 T Y Tan and U Gösele, *Appl. Phys*, **A37**, 1 (1985)
22 N K Madsen and R F Sincovec, *ACM Trans Math. Soft*, **5**, 327 (1979)
23 G Massetti, D Nobili and S Solmi, in *Semiconductor Silicon*, H R Huff and E Sirtl, Editors, PV 77-2, p 648, Electrochemical Society Softbound Proceedings Series, Princeton, NJ (1977)
24 D Nobili, A Carabelas, G Celotti, and S Solmi, *This Journal*, **130**, 922 (1983)
25 D Nobili, A Armigliato, M Finetti, and S Solmi, *J Appl. Phys*, **53**, 1484 (1982)
26 S T Dunham and R A Meade, in *Process Physics and Modeling in Semiconductor Technology*, G Srinivasan, J Plummer and S Pantelides, Editors, PV 91-4, p 287, Electrochemical Society Softbound Proceedings Series, Pennington, NJ (1991)
27 D A Antoniadis and I Moskowitz, *J Appl. Phys*, **53**, 6788 (1982)
28 E Guerrero, W Jüngling, H Pötzl, U Gösele, M Grasserbauer, and G Stingeder, *This Journal*, **133**, 2181 (1986)
29 W Richardson and B Mulvaney, *Appl. Phys Lett*, **53**, 1917 (1988)
30 G D Watkins and J W Corbett, *Phys Rev*, **134**, A1359 (1964)
31 L C Kimerling, *Inst. Phys Conf Ser*, **31**, 221 (1977)
32 I E Blount, *J Appl. Phys*, **30**, 1218 (1959)
33 S M Hu, *Phys Stat Solidi B*, **60**, 595 (1973)
34 D Mathiot and J C Pfister, *J Phys (Paris) Lett*, **43**, L-453 (1982)
35 D Mathiot and J C Pfister, *J Appl. Phys*, **66**, 970 (1989)
36 A Nylandsted Larsen, S Y Shiryaev, E Schwartz Sorensen, and P Tidemand-Petersson, *Appl. Phys. Lett*, **48**, 1805 (1986)
37 S Y Shiryaev, A Nylandsted Larsen, E Schwartz Sorensen, and P Tidemand-Petersson, *Nucl. Instrum. Methods B*, **19-20**, 507 (1987)
38 P E Anderson, A Nylandsted Larsen, P Tidemand-Petersson, and G Weyer, *Appl. Phys Lett*, **53**, 755 (1988)
39 A Nylandsted Larsen, P Tidemand-Petersson, P E Anderson, and G Weyer, *Inst Phys Conf Ser*, **95**, 499 (1989)
40 K Kyllesbech Larsen, P Gaiduk, and A Nylandsted Larsen, *MRS 1989 Fall Meeting Symposium G* (1989)
41 M Yoshida, *Jpn. J Appl. Phys*, **18**, 479 (1979)
42 M Yoshida, E Arai, H Nakamura, and Y Terunama, *J Appl. Phys*, **45**, 1498, 1899 (1974)
43 S Matsumoto and T Niimi, *Jpn J Appl. Phys*, **15**, 2077 (1976)
44 G J L Ouwerling, *The PROFILE/PROF2D User's Manual*, Delft University of Technology (1987)
45 P B Griffin and J D Plummer, *IEDM Tech. Dig*, **12**, 522 (1986)

Plasma-Enhanced Chemical Vapor Deposition of Organosilicon Thin Films from Tetraethoxysilane-Oxygen Feeds

F. Fracassi, R. d'Agostino, and P. Favia

C.N.R. Centro di Studio per la Chimica dei Plasmi, c/o Dipartimento di Chimica, Università di Bari, 70126 Bari-Italy

ABSTRACT

The composition of films deposited in RF glow discharges fed with tetraethoxysilane and oxygen mixtures has been investigated by means of *in situ* x-ray photoelectron spectroscopy and infrared spectroscopy. These results, combined with mass spectrometric investigations of the gas phase, indicate that the overall deposition consists of several concurrent heterogeneous and homogeneous reactions.

A great deal of work has been produced in the field of the plasma enhanced chemical vapor deposition (PECVD) of organosilicon compounds. The first target of these studies, initially devoted to microelectronic applications, was to gain an understanding of the deposition process in order to improve the reliability of the SiO_2 films obtained by optimizing the experimental parameters. Many organosilicon compounds, tetraethoxysilane (TEOS) in particular, can be utilized as SiO_2 precursors. Even in plasmaless environment TEOS can result in an oxide deposition by thermal decomposition (CVD) in oxidant media (*e.g.*, O_2 or N_2O) at temperatures higher than 600°C.[1] The film characteristics as well as the step coverage are usually good[1,2] but the high temperature required is very often not compatible with the device itself. To overcome this problem many studies have been done, and good deposits at lower substrate temperatures ($T < 400$°C) can now be obtained with the PECVD approach (see for instance Ref. 3-6).

A deposition mechanism has been recently proposed which agrees with the experimental evidence reported in the literature, *i.e.* the effects of power density, substrate temperature, degree of ion bombardment, etc., and also explains the dependence of the step coverage on the deposition conditions.[7-9] Even if it has not been unambiguously proven, we think this mechanism well represents the process under experimental conditions characterized by low monomer fragmentation which result in SiO_2-like films.

The proposed mechanism consists of several steps: precursor production in the plasma, which occurs for the reaction of TEOS with active species, oxygen atoms for instance; adsorption on the substrate; surface migration, which assures good step coverage; reactions of the adsorbed radicals with the active species produced by the plasma, which decrease the carbon content of the film and lead to inorganic film precursors, condensation of the inorganic radicals to form the SiO_2 network. The chemical structure of the precursors must be very close to that of TEOS, *i.e.* high organic carbon content, and therefore the fragmentation of the molecules must be kept low. Only in this case can the surface mobility of precursors be high enough to assure homogeneous surface concentration and therefore good step coverage.[7,8] For these reasons downstream deposition, with downstream TEOS admission, or very low powered glow discharges at high frequency and